Photonic-crystal surface modes found from impedances

Felix J. Lawrence,[1,*] Lindsay C. Botten,[2] Kokou B. Dossou,[2] R. C. McPhedran,[1] and C. Martijn de Sterke[1]

[1]*Centre for Ultrahigh-bandwidth Devices for Optical Systems (CUDOS), Institute for Photonics and Optical Sciences (IPOS) and School of Physics, University of Sydney, New South Wales 2006, Australia*

[2]*CUDOS and Department of Mathematical Sciences, University of Technology, Sydney, New South Wales 2007, Australia*

(Received 26 June 2010; published 30 November 2010)

We present a method for finding surface modes at interfaces between two-dimensional photonic crystals (PCs), in which the surface modes are represented as superpositions of the PCs' propagating and evanescent Bloch modes. We derive an existence condition for surface modes at an air-PC interface in terms of numerically calculated PC impedance matrices, and use the condition to find surface modes in the partial band gap of a PC. We also derive a condition for modes of a three-layer structure with two interfaces, and find both coupled surface modes and waveguide modes. We show that some waveguide modes cross the band edge and become coupled surface modes.

DOI: 10.1103/PhysRevA.82.053840 PACS number(s): 42.70.Qs, 73.20.At, 42.79.Gn, 41.20.Jb

I. INTRODUCTION

Electromagnetic surface modes have long been studied for their rich and interesting physics [1]. They are confined to an interface, in the sense that the field decays exponentially away from the interface in both directions. The most widely studied example is the surface plasmon or surface plasmon polariton, which arises at the interface between a metal and a dielectric, but these have very short propagation lengths due to loss in the metal. They have been experimentally demonstrated [2], and may even be seen with the naked eye if elastically scattered on the surface of a diffraction grating [3].

Surface states may also arise at the boundaries of two-dimensional photonic crystals (PCs), which are defined as having a periodic variation in refractive index [4]. In this paper "surface mode" refers to this variety of PC surface state, while "surface plasmon" refers exclusively to a state at the interface between a metal and a dielectric. For a surface mode at an interface between air and a PC, the field decays into the PC because of the PC's band gap, and it decays on the air side of the interface due to an effect related to total internal reflection. Since the entire structure may be made from lossless materials, surface modes can have much longer propagation lengths than surface plasmons.

PC surface modes have been experimentally demonstrated [5–8], and have been found by two general numerical approaches. The most common technique is to use a supercell [4] and directly compute the modes. With the supercell approach, the PC cannot be infinitely thick and so, in principle, there is always some coupling between surface modes on the front and back of the PC. The other widely used technique involves separately finding the modes of the two materials and calculating the surface modes from these by matching them at the interface [9–11]. This allows surface modes to be calculated for interfaces between semi-infinite structures. We take the latter approach, expressing it in terms of PC impedances [12], and generalize it to work also with structures that have a material of finite thickness sandwiched between two semi-infinite media.

Surface plasmons may be found from the poles of the transmission coefficient or of the reflection coefficient

$$r_{12} = \frac{Z_2/Z_1 - 1}{Z_2/Z_1 + 1}, \tag{1}$$

where $Z = E_\parallel/H_\parallel$ is the *wave impedance*, with $E_\parallel$ and $H_\parallel$ the field components parallel to the interface. So the condition for a surface mode to exist is that the denominator of Eq. (1) vanishes. For transverse magnetic (TM) polarization ($\mathbf{H} = H_\parallel \hat{\tau}$ with $\hat{\tau}$ parallel to the interface), for which surface plasmons may exist at an air-metal interface $Z_i = -k_{\perp i}/\omega\epsilon_i$ and so by this condition surface plasmons exist when

$$\frac{k_{\perp 1}}{\epsilon_1} = -\frac{k_{\perp 2}}{\epsilon_2}, \tag{2}$$

where $k_\perp$ is the component of the wave vector perpendicular to the interface.

In this paper we generalize the procedure for finding surface plasmons to apply to dielectric PCs and their impedances. The procedure involves finding poles of the PC analog of Eq. (1), which uses semi-analytically defined PC impedances that are generally matrices [13]. This allows us to find a condition for the existence of a PC surface mode. Section II defines our nomenclature and introduces the quantities needed to describe PCs, before the surface mode existence condition is derived in Sec. III. This is then applied to give the dispersion relation of a PC surface mode. In Sec. IV we derive a condition and give examples for the case with three media and two interfaces (e.g., a strip of PC surrounded by air on either side). We conclude in Sec. V by commenting on the usefulness of our method. The Appendix presents a convergence analysis in a typical case, illustrating the accuracy and reliability of our technique.

II. BACKGROUND THEORY AND NOMENCLATURE

We write the field in each PC in its basis of Bloch modes (including propagating and evanescent modes); this is the natural basis in which to consider transmission and reflection since each Bloch mode travels independently through its PC without scattering into other modes. Our method for finding Bloch modes is based on the semi-analytical least-squares-based method of Botten *et al.* [14] and is briefly outlined

*felix@physics.usyd.edu.au

in the following. In its present form, the method applies to two-dimensional (2D) square or triangular lattice PCs with unit cells that are up-down symmetric, which precludes the study of PCs with arbitrarily truncated unit cells. For generality we treat all media as PCs (see Fig. 1): for homogeneous dielectrics such as air, a periodicity is imposed and the material's Bloch modes are simply plane waves.

Our axes are chosen such that all PC interfaces are parallel to the x-z plane, and each PC's refractive index varies periodically in the x-y plane. We assume that both the PC structure and the electromagnetic (EM) field are invariant in the z direction; this is thus a 2D problem. In any single simulation we consider one polarization, one frequency, and one Bloch vector component k_x, the component parallel to the interface. Since the EM field components parallel to a dielectric interface are continuous across it, fixing k_x across all media ensures that we have a closed set of Bloch modes under reflection and transmission at all PC interfaces. A surface mode with propagation constant k_x may therefore be represented in each medium as a superposition of these Bloch modes.

We find the Bloch modes of each PC by diagonalizing the plane-wave transfer matrix [14], which, in turn, is found using the multipole method [15]. The transfer matrix may alternatively be found with the finite element method (FEM) [16]. The dimension of the plane-wave transfer matrix is made sufficiently large that it includes all relevant plane waves, which are the grating diffraction orders excited by the rows of holes comprising the PC. In this paper's examples, five plane-wave orders were considered in each direction in each medium; this means that the calculations typically include all relevant plane waves that decay in amplitude across a PC's unit cell by a factor of 10^6 or less. In the Appendix we give criteria illustrating how the required number of plane waves is determined and show that for our calculations five plane-wave orders are sufficient to determine surface modes accurately.

We partition the Bloch modes of each PC into modes that propagate or decay in the forward $(+y)$ direction and those that propagate or decay in the backward $(-y)$ direction. The field in a PC i is represented by a vector of forward Bloch mode amplitudes $\mathbf{c}_i^+$ and a vector of backward Bloch mode amplitudes $\mathbf{c}_i^-$ (Fig. 1).

At an interface between two PCs, each incident Bloch mode may be reflected and transmitted into many modes. Reflection and transmission coefficients must therefore become nondiagonal reflection and transmission matrices. In our previous work [12] we showed that these may be written in terms of the impedance-like matrices $\mathcal{Z}_1$ and $\mathcal{Z}_2$ of PC 1 and PC 2 [cf. Eq. (1)]

$$\mathbf{T}_{12} = \left(\mathbf{A}_{12}^T\mathbf{A}_{12} + \mathbf{I}\right)^{-1} 2\mathbf{A}_{12}^T, \tag{3a}$$

$$\mathbf{R}_{12} = \left(\mathbf{A}_{12}\mathbf{A}_{12}^T + \mathbf{I}\right)^{-1}\left(\mathbf{A}_{12}\mathbf{A}_{12}^T - \mathbf{I}\right), \tag{3b}$$

$$\mathbf{T}_{21} = \left(\mathbf{A}_{12}\mathbf{A}_{12}^T + \mathbf{I}\right)^{-1} 2\mathbf{A}_{12}, \tag{3c}$$

$$\mathbf{R}_{21} = \left(\mathbf{A}_{12}^T\mathbf{A}_{12} + \mathbf{I}\right)^{-1}\left(\mathbf{I} - \mathbf{A}_{12}^T\mathbf{A}_{12}\right), \tag{3d}$$

where $\mathbf{A}_{12} = \mathcal{Z}_1^{-1}\mathcal{Z}_2$. These equations are exact at full rank, when all relevant plane waves and Bloch modes are considered, and are otherwise least-squares-style approximations. In the Appendix we show that, for the cases in this paper, five Bloch modes and five plane waves are sufficient to obtain highly accurate results.

The impedance-like matrix $\mathcal{Z}$ is the crucial quantity that we use throughout the remainder of this paper to describe how light behaves in the PC. It is defined in terms of the PC's numerically found Bloch modes, but once the Bloch modes are known, Eq. (3) holds rigorously at full rank and becomes a least-squares approximation when the set of plane waves or Bloch modes is truncated [12].

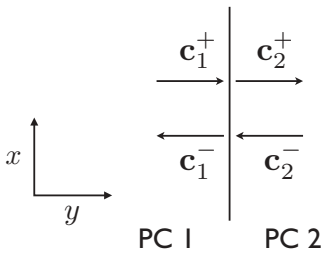

FIG. 1. Schematic of a two PC interface, with incoming and outgoing Bloch vectors.

III. SINGLE INTERFACE SURFACE MODES

We derive a necessary and sufficient condition for the existence of a PC surface mode in a similar way to how the surface plasmon condition Eq. (2) may be derived: we look for poles of the reflection matrices. We work in the PCs' Bloch bases, with notation as in Fig. 1. Poles of matrices imply infinite eigenvalues; to avoid the ensuing numerical instabilities, we instead calculate the inverse of these matrices and look for zero eigenvalues. The condition for a surface mode, in this form, is then the pair of homogenous equations

$$\mathbf{R}_{12}^{-1}\mathbf{c}_1^- = \mathbf{c}_1^+ = \mathbf{0}, \tag{4a}$$

$$\mathbf{R}_{21}^{-1}\mathbf{c}_2^+ = \mathbf{c}_2^- = \mathbf{0}. \tag{4b}$$

Equation (4) constitutes a necessary condition because a surface mode has zero incoming field (i.e., $\mathbf{c}_1^+ = \mathbf{0}$ and $\mathbf{c}_2^- = \mathbf{0}$) and nonzero outgoing field (i.e., $\mathbf{c}_1^- \neq \mathbf{0}$ and $\mathbf{c}_2^+ \neq \mathbf{0}$), so $\mathbf{R}_{12}^{-1}$ and $\mathbf{R}_{21}^{-1}$ must be singular. Possible issues of degeneracy are resolved by studying the null space, for which the singular value decomposition is a useful tool. They also constitute a sufficient condition because the null vectors of $\mathbf{R}_{12}^{-1}$ and $\mathbf{R}_{21}^{-1}$ are valid outgoing fields without incoming fields, which is the definition of a surface mode.

To find the source of the singularity, consider the expressions for $\mathbf{R}_{12}$ and $\mathbf{R}_{21}$ in Eqs. (3b) and (3d). The impedance ratio $\mathbf{A}_{12}\mathbf{A}_{12}^T$ does not have an infinite eigenvalue since that would imply that one of the Bloch modes could not be normalized and had zero or an infinite field associated with it. Therefore to satisfy Eqs. (4a) and (4b), $(\mathbf{A}_{12}\mathbf{A}_{12}^T + \mathbf{I})$ and $(\mathbf{A}_{12}^T\mathbf{A}_{12} + \mathbf{I})$ must have a zero eigenvalue. Looking again at Eq. (3), this implies that surface modes are tied to poles of the reflection and transmission matrices in both directions. This is consistent with the condition used by Enoch *et al.* [10], that of a pole in the scattering matrix determinant; and the condition of Che and Li [11], that $\det(\mathbf{S}_{11}) = \mathbf{0}$, where $\mathbf{S}_{11}$ is the submatrix of the scattering matrix that maps $\mathbf{c}_2^+$ to $\mathbf{c}_1^+$.

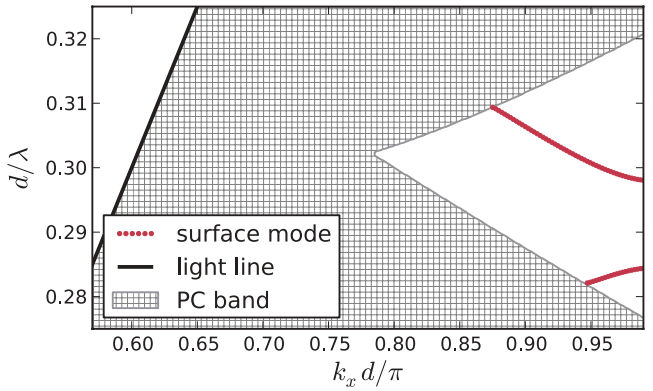

FIG. 2. (Color online) Projected band structure of surface modes at an air-PC interface. Only the region below the light line is considered.

So to find the surface modes of a structure, we scan frequency and vary k_x in search of cases where $(\mathbf{A}_{12}\mathbf{A}_{12}^T + \mathbf{I})$ has a zero eigenvalue. Thus by searching frequency-k_x space we construct the projected band structure of the interface. The eigenvector associated with each zero eigenvalue is $\mathbf{c}_1^-$ for the surface mode, as may be seen from Eq. (4a). And from Eq. (4b) we see that the amplitudes of PC 2's Bloch modes, $\mathbf{c}_2^+$, is the eigenvector corresponding to the zero eigenvalue of $(\mathbf{A}_{12}^T\mathbf{A}_{12} + \mathbf{I})$. Knowing the Bloch mode amplitudes $\mathbf{c}_1^-$ and $\mathbf{c}_2^+$ lets us find and plot the surface mode's field.

We now apply this method to find the surface modes at the interface between air and a semi-infinite PC. The PC has a triangular lattice of air holes of radius $0.25d$, with lattice constant d, in a dielectric background with $n = 2.86$. We look for surface modes in the $\mathbf{E} = E_z\hat{\mathbf{z}}$ polarization; surface plasmons do not exist in this polarization since this would require a medium with negative permeability.

Surface modes only occur where there are no propagating modes in either material; since one of the media is air, we only look for surface modes below the light line [4]. We scan over frequency and k_x for eigenvalues of $(\mathbf{A}_{12}^T\mathbf{A}_{12} + \mathbf{I})$ that have magnitudes below our accuracy goal of 10^{-12} and find two surface modes in a partial band gap. The resulting projected band structure is plotted in Fig. 2.

The real and imaginary parts of the smallest eigenvalue ψ of $(\mathbf{A}_{12}^T\mathbf{A}_{12} + \mathbf{I})$ are plotted in Fig. 3 for $d/\lambda = 0.3$. The surface mode is found where the real part crosses the x axis; within the band gap $\mathrm{Im}(\psi)$ is essentially zero. This eigenvalue appears to have no physical significance other than indicating whether $(\mathbf{A}_{12}^T\mathbf{A}_{12} + \mathbf{I})$ is singular. This result was obtained considering five Bloch modes and five plane waves; a convergence analysis presented in the Appendix shows that this approximation is highly accurate.

The field in the PC (shown in Fig. 4) is essentially a superposition of the two most slowly decaying Bloch modes; for $d/\lambda = 0.3$, the moduli of the Bloch amplitudes $\mathbf{c}_2^+$ are 0.43, 0.90, 4.4×10^{-3}, 7.7×10^{-3}, and 1.4×10^{-4}, where the corresponding Bloch factors (eigenvalues of the transfer matrix) have moduli 0.65, 0.64, 1.0×10^{-3}, 7.9×10^{-4}, and 2.7×10^{-6}, respectively. Close to the interface, the second Bloch mode dominates, but deep in the PC the first Bloch mode becomes responsible for most of the field because it decays

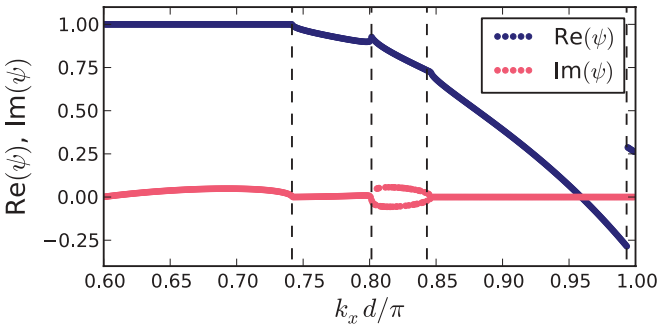

FIG. 3. (Color online) Real and imaginary parts of the smallest eigenvalue of $(\mathbf{A}_{12}^T\mathbf{A}_{12} + \mathbf{I})$, for $d/\lambda = 0.3$. Surface modes occur when this eigenvalue is exactly zero. The discontinuities in slope occur where two or more eigenvalues have equal moduli.

slightly more slowly. Similarly, on the air side of the interface most of the field is due to the two most slowly decaying plane waves; the transition region where the two plane waves are of comparable amplitude and so interference is clearly visible in Fig. 4(b). The slowest decaying plane wave has a decay length (to a factor $1/e$ amplitude) of $0.23\sqrt{3/2}d$.

Since the field on both sides of the interface is a superposition of two modes with different decay factors, the field does not exponentially decay away from the interface, and

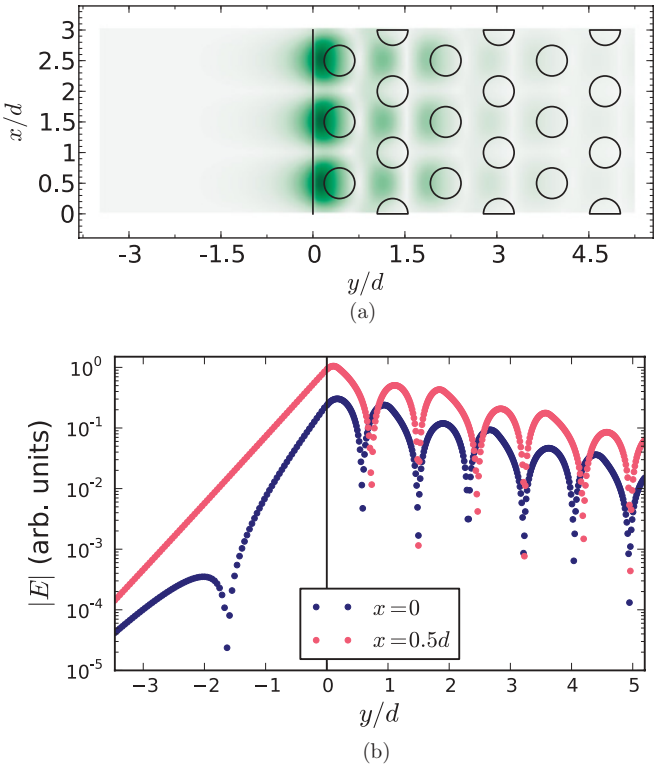

FIG. 4. (Color online) Modulus of the E field for the surface mode at $d/\lambda = 0.3$ and $k_x = 0.959\pi/d$; air is on the left of the vertical line, PC is on the right. Two horizontal cuts through (a) are shown in (b); the $x = 0$ cut is along the lower edge of (a), and the $x = 0.5d$ cut bisects one of the three PC holes nearest the interface. The $x = 0$ cut shows two exponential decay regimes in air, which is evidence that one evanescent plane wave dominates near the interface and another dominates away from it.

so the surface mode may not faithfully be approximated by a surface plasmon. In other words, this PC's behavior may not be reproduced by any uniform medium; no effective permittivity or permeability that may be ascribed to the PC could predict this surface mode.

IV. DOUBLE INTERFACE SURFACE MODES

Another much-studied configuration in the surface plasmon literature is that of thin metallic slabs in air (or another dielectric). Such structures can support surface plasmons on both faces of the metallic slab, which couple [17]. These surface states are long-range or short-range surface plasmons, depending on their symmetry. In this section we explore nonmetallic PC analogs to long- and short-range surface plasmons; we consider structures with three media and two interfaces, either of which may or may not be capable of supporting a surface mode.

Such structures have previously been studied by Enoch *et al.* [10], who investigated a dielectric-PC-dielectric structure analogous to the dielectric-metal-dielectric structures on which long- and short-range surface plasmons have been observed. Their PC region is fixed at 18 periods thick, so the coupling between interfaces is minimal. Choi *et al.* [18] investigated a PC-air-PC structure. In our examples we consider an air-PC-air structure, but the theory developed is general and also applies to other structures, including PC waveguides.

The three media, which for generality we consider to be PCs, are arranged as in Fig. 5. $\mathbf{\Lambda}_+ = \mathrm{diag}(\mu^s_{f,i})$ and $\mathbf{\Lambda}_- = \mathrm{diag}(\mu^{-s}_{b,i})$, where $\mu_{f,i}$ and $\mu_{b,i}$ are, respectively, PC 2's forward and backward Bloch factors (eigenvalues) and s is PC 2's width.

To find the condition for a surface mode, we set the incoming field vectors $\mathbf{c}_1^+$ and $\mathbf{c}_3^-$ to zero and derive

$$\mathbf{c}_2^+ = \mathbf{R}_{21}\mathbf{\Lambda}_-\mathbf{c}'^-_2, \tag{5a}$$

$$\mathbf{c}'^-_2 = \mathbf{R}_{23}\mathbf{\Lambda}_+\mathbf{c}_2^+, \tag{5b}$$

which leads to

$$(\mathbf{R}_{21}\mathbf{\Lambda}_-\mathbf{R}_{23}\mathbf{\Lambda}_+ - \mathbf{I})\mathbf{c}_2^+ = \mathbf{0}. \tag{6}$$

This expression is closely related to the familiar waveguide phase condition; it is satisfied by conventional waveguide modes. However, it is also satisfied by surface modes, which decay inside PC 2 away from the interfaces. For surface modes, the entries of the diagonal matrices $\mathbf{\Lambda}_+$ and $\mathbf{\Lambda}_-$ all have magnitude less than unity; this is balanced by reflection matrices that increase field amplitude upon reflection.

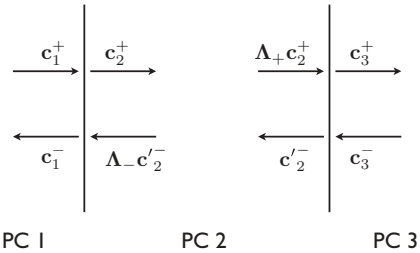

FIG. 5. Schematic of a three PC (double interface) structure, with Bloch vectors $\mathbf{c}$.

In deriving Eq. (6), we neglected terms due to the incoming field vectors $\mathbf{c}_1^+$ and $\mathbf{c}_3^-$, which both vanish for a surface mode. The more general form of Eq. (5a) is $\mathbf{c}_2^+ = \mathbf{R}_{21}\mathbf{\Lambda}_-\mathbf{c}'^-_2 + \mathbf{T}_{12}\mathbf{c}_1^+$. In Sec. III, we found surface modes occurring at poles of the reflection and transmission matrices (i.e., modes where $\mathbf{T}_{12}\mathbf{c}_1^+$ was nonzero even when $\mathbf{c}_1^+ = \mathbf{0}$). We now consider whether the possibility of a pole in the transmission matrix can invalidate Eq. (5a).

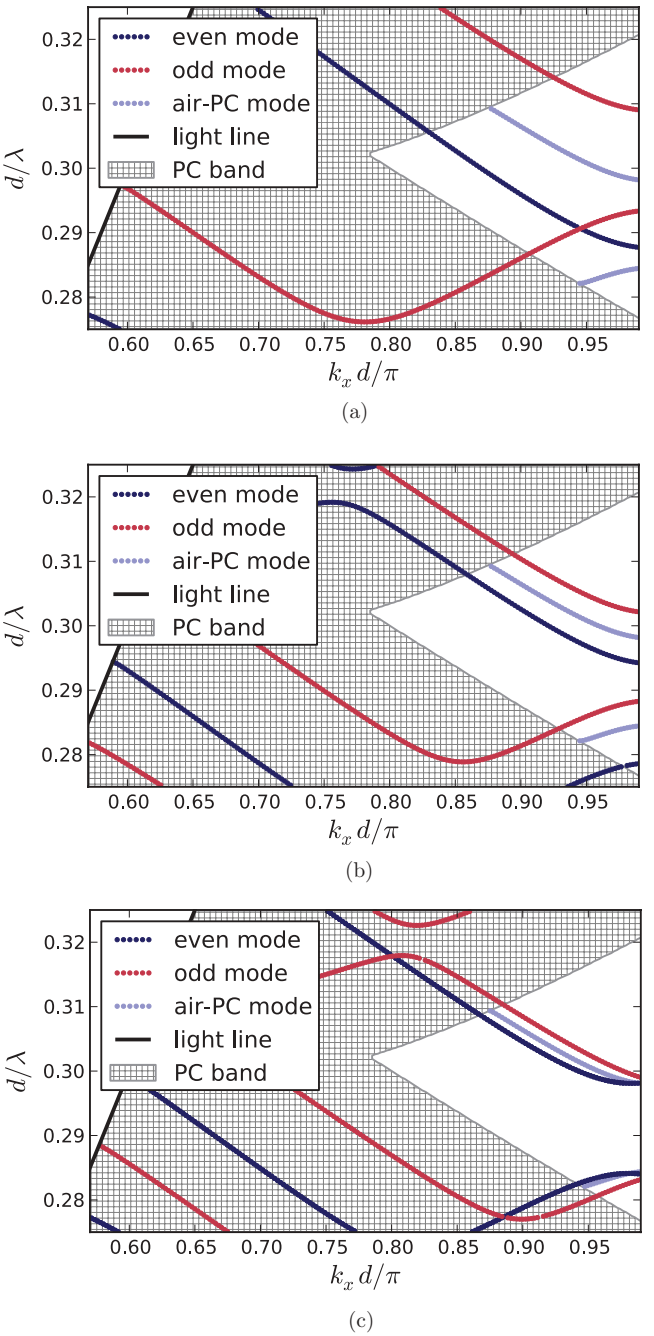

FIG. 6. (Color online) Projected band structure of surface modes (dark blue and midtone red) of an air-PC-air structure with (a) three, (b) five, and (c) six periods of PC. The projected band structure of the surface modes at the corresponding air-PC interface is shown for reference in light blue.

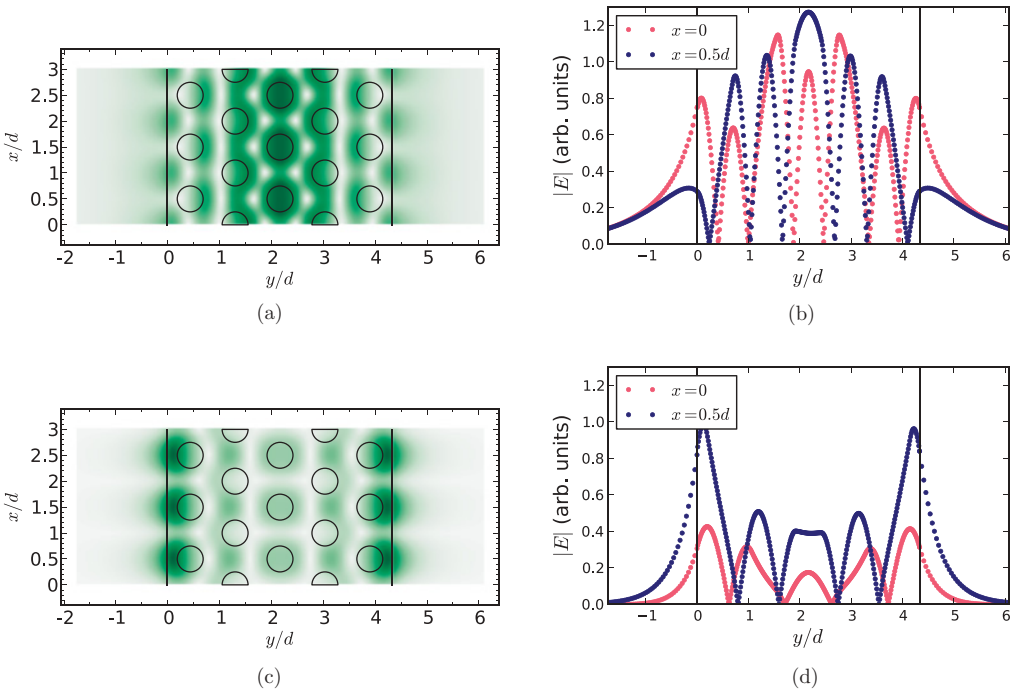

FIG. 7. (Color online) Field strength $|E|$ for an even mode of an air-PC-air structure with five periods of PC [see Fig. 6(b)]: (a) and (b) at $d/\lambda = 0.318$, $k_x = 0.715\pi/d$, in the PC's band; (c) and (d) at $d/\lambda = 0.299$, $k_x = 0.927\pi/d$, in the PC band gap.

As we saw in Sec. III, poles occur when $\mathbf{c}_1^-$ lies in the null space of $(\mathbf{A}_{12}\mathbf{A}_{12}^T + \mathbf{I})$. Considering the field at the PC 1-PC 2 interface, we may write

$$(\mathbf{A}_{12}\mathbf{A}_{12}^T + \mathbf{I})\mathbf{c}_1^- = (\mathbf{A}_{12}\mathbf{A}_{12}^T - \mathbf{I})\mathbf{c}_1^+ + 2\mathbf{A}_{12}\mathbf{\Lambda}_-\mathbf{c'}_2^-, \quad (7)$$

and see that if $\mathbf{c}_1^-$ is in the null space of $(\mathbf{A}_{12}\mathbf{A}_{12}^T + \mathbf{I})$, the necessary condition for a pole, then $(\mathbf{A}_{12}\mathbf{A}_{12}^T + \mathbf{I})\mathbf{c}_1^- = \mathbf{0}$. Furthermore $\mathbf{c}_1^+ = \mathbf{0}$ for a surface mode, resulting in $2\mathbf{A}_{12}\mathbf{\Lambda}_-\mathbf{c'}_2^- = \mathbf{0}$. This implies that no field from the PC 2-PC 3 interface reaches the PC 1-PC 2 interface, which is not physical. Therefore there can be no double interface surface modes when there are poles in the transmission matrices and Eq. (6) is both a sufficient and necessary condition for a double interface surface mode.

Of particular interest is the symmetric case, where PC 1 and PC 3 are the same material. Then $\mathbf{R}_{21} = \mathbf{R}_{23}$ and we can factorize Eq. (6). We use the relation $\mathbf{\Lambda}_- = e^{i\pi k_x s d}\mathbf{\Lambda}_+$, where s is the number of rows of holes in PC 2, to write

$$(\mathbf{R}_{21}\mathbf{\Lambda}_+ e^{i\pi k_x s d/2} - \mathbf{I})(\mathbf{R}_{21}\mathbf{\Lambda}_+ e^{i\pi k_x s d/2} + \mathbf{I})\mathbf{c}_2^+ = \mathbf{0}. \quad (8)$$

Comparing this to Eq. (5), two solutions are apparent: an even solution, where $\mathbf{c'}_2^- = e^{-i\pi k_x s d/2}\mathbf{c}_2^+$ and an odd solution for which $\mathbf{c'}_2^- = -e^{-i\pi k_x s d/2}\mathbf{c}_2^+$. Note that this phase shift of $\pm e^{-i\pi k_x s d/2}$ is measured between points separated by s lattice vectors, so for triangular lattices these points have different x values since that lattice vector is not parallel to the y axis.

We now apply this method to find the modes of a structure in which PC 1 and PC 3 are vacuum and PC 2 is the PC studied in Sec. III. We search for eigenvectors of $\mathbf{R}_{21}\mathbf{\Lambda}_+ e^{i\pi k_x s d/2}$ that have an eigenvalue ψ within an accuracy range 10^{-6} of ± 1, for $\mathbf{E} = E_z\hat{\mathbf{z}}$ polarized light. The modes found when PC 2 is three, five, and six rows of holes thick are shown in Fig. 6.

The striking difference between the single interface surface modes of Sec. III and the double interface modes in Fig. 6 is that the double interface modes cross the PC's band edge, as reported for the thick PC limit by Enoch *et al.* [10]. As previously discussed, single interface surface modes cannot exist in band, as energy is inevitably radiated away [4]. When a second interface is present, in-band waveguide solutions arise for Eq. (6), in addition to band-gap surface mode solutions.

The character of a mode changes across the band edge: in the band gap, the field envelope must decay toward the center of the PC slab since all its constituent Bloch modes are evanescent. In band, this restriction does not apply. Figure 7 shows two cuts through the field of an even mode of the air-5 period PC-air structure of Fig. 6(b). The difference between the in-band waveguide mode [Figs. 7(a) and 7(b)] and the band-gap surface mode [Figs. 7(c) and 7(d)] is readily apparent; the surface mode's field unambiguously decays toward the center of the PC region, whereas the waveguide mode has a large field along the middle of the PC. There is a smooth transition between these two kinds of mode: near the band edge, the waveguide mode adopts the shape of the surface mode. The moduli of the elements of $\mathbf{c}_2^+$ for each mode vary continuously, even across the band edge, and likewise there is no sudden change in the field profile as the band edge is crossed.

The introduction of a second interface splits the single interface surface mode into an even mode and an odd mode. As the thickness of PC 2 is increased, we see from Fig. 6 that these modes' dispersion relations converge, approaching that of the single interface surface mode. This behavior makes physical sense, as the interfaces become increasingly decoupled as PC 2's thickness increases. Furthermore as

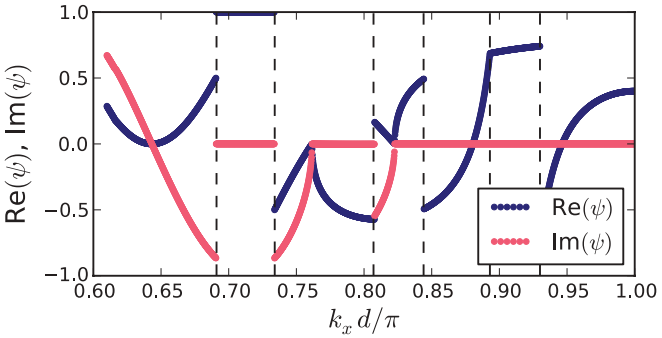

FIG. 8. (Color online) Real and imaginary parts of the smallest eigenvalue ψ of $\mathbf{R}_{21}\mathbf{\Lambda}_+ e^{i\pi k_x sd/2} \pm \mathbf{I}$ at $d/\lambda = 0.305$ for the air-PC-air structure used in Fig. 6(b). The condition for a surface mode or waveguide mode is $\psi = 0$. Discontinuities occur where two or more eigenvalues have equal moduli.

PC 2's thickness increases, the magnitude of the entries of $\mathbf{\Lambda}_+$ decrease exponentially. Since $\mathbf{R}_{21}^{-1}\mathbf{c}_2^+ = \pm e^{i\pi k_x sd/2}\mathbf{\Lambda}_+\mathbf{c}_2^+$, as PC 2's thickness becomes infinite, $\mathbf{\Lambda}_+ \to \mathbf{0}$. Therefore $\mathbf{R}_{21}^{-1}$ must become singular, which is precisely the condition for a single interface surface mode.

Unlike the PC-air-PC structure studied by Choi *et al.* [18], Fig. 6 shows that, in our case, the lower-frequency mode does not always have even parity. For our configuration, when the PC is an even number of periods thick the lowest-frequency surface mode is odd, and vice versa; we have checked this for PCs from four to eight periods thick. This behavior is equivalent to that previously observed in coupled PC waveguides [19]. For thinner structures, in which the interfaces are strongly coupled, the lower air-PC mode does not split into two surface modes.

Numerically finding solutions to Eq. (8) is sometimes more difficult than the single-mode case, because the eigenvalue ψ that must be minimized can vary strongly with frequency and k_x. For example, $\psi(k_x)$ is shown in Fig. 8 at $d/\lambda = 0.305$ for the 5 period thick PC of Fig. 6(b). This function has several discontinuities and is less well behaved than the equivalent function for the single interface, shown in Fig. 3. The discontinuities occur where the two smallest eigenvalues have equal magnitude. Discontinuities close to a zero can cause a root-finder to miss valid solutions; this manifests as a gap in the dispersion relation and can be avoided by instead searching for a zero determinant. This measure was necessary to obtain certain points on the even mode dispersion relations in Fig. 6(c). Furthermore in Fig. 8 there are cusps near $k_x = 0.76\pi/d$ and $k_x = 0.82\pi/d$, where the number of propagating Bloch modes changes. These anomalies are extremely localized—for the $k_x \simeq 0.76\pi/d$ anomaly, $|\psi| < 10^{-5}$ over a domain of size $\Delta k_x < 10^{-10}\pi/d$—so the anomalies are of no practical importance and are therefore ignored in Fig. 6.

The numerical issues in finding modes arise because to find a k_x for a given frequency (or vice versa) that supports a mode, a numerical search must be performed to find a k_x such that $|\psi| = 0$. To find a projected band structure like those in Fig. 6, we must scan over frequency and k_x, a 2D search. Our approach is to do a coarse search over the entire parameter space, then to use a root finder to check local minima for zeros. The information calculated for each PC (i.e., its impedance and Bloch factor) in the coarse search is independent of the overall PC 1-PC 2-PC 3 structure. This means that the hard work in generating Figs. 6(a), 6(b), and 6(c) only needs to be done once: with the PCs' impedances known, the coarse search becomes simply a matter of manipulating known 3×3 or 5×5 matrices.

Supercell methods [4] require only a one-dimensional (1D) search because for each frequency, all appropriate k_x may be found directly from a single FEM (or other) computation. The main downside to supercell methods is that coupling occurs between supercells; the supercell must be made large to minimize this, which adds computation time. The minimal supercell size depends on the decay rates in the outermost media, which depend on k_x and may not be known in advance. Our impedance method does not suffer from this problem: the outer media are truly semi-infinite and the computational domain is small since we compute each PC's Bloch modes using a single unit cell. Our Bloch mode method also provides additional insight into the field structure that supercell methods do not provide.

V. DISCUSSION AND CONCLUSION

In Sec. IV we generalize the principles from Sec. III to investigate modes that propagate along a three-layer structure. The results given in Sec. IV are for an air-PC-air structure, which was chosen so that in the partial band gap the surface modes are analogous to long-range surface plasmons. However, the derived equations are quite general: Eq. (6) may be used to find the modes of any three-layer structure and Eq. (8) may be applied to any structure of the form PC 1-PC 2-PC 1, which includes many PC waveguides. Unlike supercell methods, our approach allows the field of a waveguide mode to be expressed as a superposition of Bloch modes in each of the structure's constituent PCs. This allows a deeper understanding of the waveguide mode and how it decays in the confining media.

The method developed in Sec. IV may be extended to treat structures with more than three media; this simply requires further use of the transfer matrix method used in deriving Eqs. (5) and (6). Such an approach could be used to find the modes of coupled PC waveguides, or of more complicated PC waveguide structures where the rows of holes nearest the central guiding region have been modified.

In conclusion, we have developed a method of finding surface modes on two- and three-layer structures. The condition for surface modes on a single interface is that the Bloch mode reflection matrix has an infinite eigenvalue, which is analogous to the condition for a surface plasmon on an air-metal interface, and we provide an equivalent condition in terms of PC impedances. Our PC impedance condition is more numerically suitable than the reflection matrix formulation, since we isolate the matrix responsible for the zero eigenvalues that correspond to physically significant solutions. The analysis of an example shows that a single surface mode may involve two Bloch modes with different decay rates, on both sides of the interface.

The condition for surface and waveguide modes on a three-layer structure [Eq. (6)] is similar to that for a dielectric

TABLE I. k_x for a surface mode is repeatedly calculated, varying the number of Bloch modes (vertical axis) and plane waves (horizontal axis) used in the calculation. The table shows the difference of these calculated k_x from 0.957 765 360 815 $104\pi/d$, the k_x for the surface mode calculated with 11 forward and 11 backward Bloch modes and plane waves.

	Number of plane waves				
	3	5	7	9	11
2	3.2×10^{-5}	1.1×10^{-4}	8.0×10^{-5}	1.1×10^{-4}	8.0×10^{-5}
3	6.1×10^{-5}	1.4×10^{-4}	1.3×10^{-5}	1.4×10^{-4}	1.3×10^{-5}
4		1.1×10^{-7}	3.6×10^{-8}	1.8×10^{-7}	3.4×10^{-8}
5		4.4×10^{-8}	1.8×10^{-7}	2.4×10^{-7}	1.8×10^{-7}
6			8.7×10^{-10}	2.8×10^{-10}	7.6×10^{-10}
7			4.8×10^{-10}	9.5×10^{-10}	1.3×10^{-9}
8				4.2×10^{-12}	4.8×10^{-12}
9				4.8×10^{-12}	3.0×10^{-12}
10					1.0×10^{-14}

TABLE II. k_x for a surface mode is repeatedly calculated, varying the number of Bloch modes and plane waves, as in Table I. The eigenvalue of $(\mathbf{A}_{12}^T\mathbf{A}_{12} + \mathbf{I})$, which should be zero for a surface mode, is then calculated for each k_x using 11 Bloch modes and 11 plane waves.

	Number of plane waves				
	3	5	7	9	11
2	2.4×10^{-4}	8.2×10^{-4}	6.0×10^{-4}	8.2×10^{-4}	6.0×10^{-4}
3	4.6×10^{-4}	1.1×10^{-3}	9.8×10^{-5}	1.1×10^{-3}	9.8×10^{-5}
4		8.1×10^{-7}	2.7×10^{-7}	1.3×10^{-6}	2.6×10^{-7}
5		3.3×10^{-7}	1.4×10^{-6}	1.8×10^{-6}	1.4×10^{-6}
6			6.6×10^{-9}	2.1×10^{-9}	5.8×10^{-9}
7			3.6×10^{-9}	7.2×10^{-9}	1.0×10^{-8}
8				3.2×10^{-11}	3.7×10^{-11}
9				3.7×10^{-11}	2.2×10^{-11}
10					8.1×10^{-14}
11					9.8×10^{-15}

waveguide. We find that some of the waveguide modes of an air-PC-air structure cross the band edge and continue into the partial band gap, becoming surface modes with mode profiles that decay toward the center of the PC region.

ACKNOWLEDGMENTS

This work was produced with the assistance of the Australian Research Council (ARC). CUDOS (the Centre for Ultrahigh-bandwidth Devices for Optical Systems) is an ARC Centre of Excellence.

APPENDIX: COMPLETENESS AND CONVERGENCE

In Sec. II we noted that for the calculations in this paper we represent the field by five forward and five backward propagating and decaying plane-wave diffraction orders. We now explore the validity of this truncation by presenting a convergence analysis for one data point of our results.

As our method is based on that of Botten *et al.* [14], there are two fundamental approximations made in representing field in the PC: the countably infinite set of plane-wave grating diffraction orders is truncated to a finite size, and the set of Bloch modes found by diagonalizing the plane-wave transfer matrix is also truncated. The total set of Bloch modes is complete [20], so without such truncations arbitrary fields in the PC could be exactly represented as superpositions of Bloch modes. We have shown in previous work [13] that there is a minimum number of Bloch modes necessary to provide realistic results for PC reflection coefficients, and that beyond this, convergence with increasing mode number is very rapid. This feature carries over to the study of surface modes, given their close connection to reflection matrices. In this Appendix we further investigate the effect of these truncations on our results for the k_x of a surface mode on an air-PC interface found at a particular frequency. There are further numerical inaccuracies arising from the calculation of plane-wave scattering, but these are comprehensively treated elsewhere [21].

As mentioned in Sec. III, we consider the interface between air and a triangular lattice PC with air holes of radius $0.25d$, where d is the lattice constant, and the background refractive index is $n = 2.86$. The air-PC interface is in the y-z plane. Light is polarized with $\mathbf{E} = E_z\hat{\mathbf{z}}$ and has the frequency $d/\lambda = 0.3$.

We repeatedly apply a root finder to determine the k_x for a surface mode, varying the number of plane-wave orders and the number of Bloch modes. Table I shows how the calculated k_x varies with these parameters. The results converge quickly as the size of the Bloch basis increases. There is negligible difference (4.4×10^{-8}) between the five plane wave and Bloch mode calculation (the approximation used throughout this paper) and the 11 plane wave and Bloch mode calculation. Since the Bloch modes are orthogonal and represented in terms of plane-wave orders, every calculation has more plane-wave orders than Bloch modes. When using a single Bloch mode, the surface mode is not found.

In Sec. III it was established that surface modes occur when $(\mathbf{A}_{12}^T\mathbf{A}_{12} + \mathbf{I})$ has a zero eigenvalue. Table II gives the magnitude of the smallest eigenvalue associated with each k_x in Table I, as calculated with 11 Bloch modes and plane waves. It shows good convergence thereby demonstrating that our work has a solid foundation.

[1] A. D. Boardman, *Electromagnetic Surface Modes* (Wiley, New York, 1982).
[2] R. Ulrich and M. Tacke, Appl. Phys. Lett. **22**, 251 (1973).
[3] M. C. Hutley, *Diffraction Gratings* (Academic Press, New York, 1982).
[4] R. D. Meade, K. D. Brommer, A. M. Rappe, and J. D. Joannopoulos, Phys. Rev. B **44**, 10961 (1991).
[5] W. M. Robertson, G. Arjavalingam, R. D. Meade, K. D. Brommer, A. M. Rappe, and J. D. Joannopoulos, Opt. Lett. **18**, 528 (1993).

[6] Y. A. Vlasov, N. Moll, and S. J. McNab, Opt. Lett. **29**, 2175 (2004).
[7] B. Wang, W. Dai, A. Fang, L. Zhang, G. Tuttle, T. Koschny, and C. M. Soukoulis, Phys. Rev. B **74**, 195104 (2006).
[8] K. Ishizaki and S. Noda, Nature (London) **460**, 367 (2009).
[9] J. M. Elson and P. Tran, Phys. Rev. B **54**, 1711 (1996).
[10] S. Enoch, E. Popov, and N. Bonod, Phys. Rev. B **72**, 155101 (2005).
[11] M. Che and Z. Y. Li, J. Opt. Soc. Am. A **25**, 2177 (2008).
[12] F. J. Lawrence, L. C. Botten, K. B. Dossou, C. M. de Sterke, and R. C. McPhedran, Phys. Rev. A **80**, 023826 (2009).
[13] F. J. Lawrence, L. C. Botten, K. B. Dossou, and C. M. de Sterke, Appl. Phys. Lett. **93**, 121114 (2008).
[14] L. C. Botten, T. P. White, A. A. Asatryan, T. N. Langtry, C. M. de Sterke, and R. C. McPhedran, Phys. Rev. E **70**, 056606 (2004).
[15] L. C. Botten, N.-A. P. Nicorovici, A. A. Asatryan, R. C. McPhedran, C. M. de Sterke, and P. A. Robinson, J. Opt. Soc. Am. A **17**, 2165 (2000).
[16] K. Dossou, M. A. Byrne, and L. C. Botten, J. Comput. Phys. **219**, 120 (2006).
[17] F. Yang, J. R. Sambles, and G. W. Bradberry, Phys. Rev. B **44**, 5855 (1991).
[18] H.-G. Choi, S. S. Oh, S.-G. Lee, M.-W. Kim, J.-E. Kim, H. Y. Park, and C.-S. Kee, J. Appl. Phys. **100**, 123105 (2006).
[19] C. M. de Sterke, L. C. Botten, A. A. Asatryan, T. P. White, and R. C. McPhedran, Opt. Lett. **29**, 1384 (2004).
[20] C. H. Wilcox, Journal d'analyse mathématique **33**, 146 (1978).
[21] R. C. McPhedran, N. A. Nicorovici, L. C. Botten, and K. A. Grubits, J. Math. Phys. **41**, 7808 (2000).